Title

Cul4-Ddb1 ubiquitin ligases facilitate DNA replication-coupled sister chromatid cohesion through regulation of cohesin acetyltransferase Esco2

Authors

Haitao Sun, Jiaxin Zhang, Jingjing Zhang, Zhen Li, Qinhong Cao*, Huiqiang Lou*

Affiliations

Beijing Advanced Innovation Center for Food Nutrition and Human Health and State Key Laboratory of Agro-Biotechnology, College of Biological Sciences, China Agricultural University, Beijing, China

*To whom correspondence should be addressed: Qinhong Cao, Tel/Fax: 8610-62731071; E-mail: caoqinhong@cau.edu.cn(QC); and Huiqiang Lou, Tel/Fax: 8610-62734504; E-mail: lou@cau.edu.cn(HL).

Run title

Esco2 is linked to fork by CRL4 ligases and PCNA

Abstract

Cohesin acetyltransferases Esco1 and Esco2 play a vital role in establishing sister chromatid cohesion. How Esco1 and Esco2 are controlled to achieve this in a DNA replication-coupled manner remains unclear in higher eukaryotes. Here we show that Cul4-RING ligases (CRL4s) play a critical role in sister chromatid cohesion in human cells. Depletion of Cul4A, Cul4B or Ddb1 subunits substantially reduces normal cohesion efficiency. We also show that Mms22L, a vertebrate ortholog of yeast Mms22, is one of Ddb1 and Cul4-associated factors (DCAFs) involved in cohesion. Several lines of evidence suggest a selective interaction of CRL4s with Esco2, but not Esco1. Depletion of either CRL4s or Esco2 causes a defect in Smc3 acetylation which can be rescued by HDAC8 inhibition. More importantly, both CRL4s and PCNA act as mediators for efficiently stabilizing Esco2 on chromatin and catalyzing Smc3 acetylation. Taken together, we propose an evolutionarily conserved mechanism in which CRL4s and PCNA regulate Esco2-dependent establishment of sister chromatid cohesion.

Author summary

We identified human Mms22L as a substrate specific adaptor of Cul4- Ddb1 E3 ubiquitin ligase. Downregulation of Cul4A, Cul4B or Ddb1 subunit causes reduction of acetylated Smc3, via interaction with Esco2 acetyltransferase, and then impairs sister chromatid cohesion in 293T cells. We found functional complementation between Cul4- Ddb1- Mms22L E3 ligase and Esco2 in Smc3 acetylation and sister chromatid cohesion. Interestingly, both Cul4- Ddb1 E3 ubiquitin ligase and PCNA contribute to Esco2 mediated Smc3 acetylation. To summarise, we demonstrated an evolutionarily conserved mechanism in which Cul4- Ddb1 E3 ubiquitin ligases and PCNA regulate Esco2-dependent establishment of sister chromatid cohesion.

Introduction

Faithful inheritance of the genetic information requires precise chromatin replication and separation of sister chromatids into two daughter cells. To ensure accurate chromosome segregation in eukaryotic cells, a pair of sister chromatids should be aligned properly and held together by a cohesin complex from S phase to anaphase [1-6]. The cohesin complex is a four-subunit ring conserved from yeast to human. In human mitotic cells, cohesin is composed of Smc1, Smc3, Rad21 (Scc1/Mcd1 in yeast) and SA1 or SA2 (Scc3 in yeast) [2, 7-10].

Cohesin is widely believed to have distinct statuses according to its association with chromatin during the cell cycle. In G_1 phase, it is loaded loosely onto chromatin (i.e., non-cohesive status) [11]. As cells proceed into S phase, cohesin binds more tightly to hold sister chromatids together (i.e. cohesive status), and this transition is called the establishment of sister chromatid cohesion [5, 12]. Although the structural bases of this transition remain enigmatic, it has been shown in yeast (*Saccharomyces cerevisiae*) to depend on an essential cohesin acetyltransferase, Eco1 [13-15]. Eco1 triggers cohesion establishment during S phase through counteracting the opposing activity of Rad61 (WAPL in human) [16]. The essential substrate of Eco1 has been demonstrated to be Smc3 [13].

Cohesion is established in a DNA replication-coupled manner [12, 17, 18]. To achieve this, the activity of Eco1 is controlled concomitantly with DNA replication by two independent mechanisms. First, Eco1 contains a canonical PIP (PCNA interaction peptide) box, which mediates its interaction with PCNA, the multivalent-platform of

DNA replisome [19]. Second, a member of the cullin-RING E3 ligases (CRLs) Rtt101-Mms1, associates with the replication fork and facilitates Smc3 acetylation through direct association between Eco1 and the substrate receptor component of the ligase, Mms22 [20].

CRLs constitute the largest ubiquitin ligase family in eukaryotes. They are modular assemblies consisting of a Cullin scaffold in complex with an adapter and distinct ligase substrate receptors, giving rise to many combinatorial possibilities. There are three cullins in budding yeast (Cul1, 3 and 8) and six in human (Cul1, 2, 3, 4A, 4B and 5) [21]. Cul8, also known as Rtt101, is unique to budding yeast, but shows low sequence similarity with Cul4. Nevertheless, the Rtt101 adaptor Mms1 is highly homologous to human Ddb1 adapter of Cul4, and Rtt101-Mms1 performs similar functions to Cul4-Ddb1 ligases in other organisms [22]. The human genome encodes two Cul4 paralogs, Cul4A and Cul4B, sharing 80% sequence identity aside from Cul4B having an extended N-terminus containing a nuclear localization signal (NLS) [23]. Both Cul4A and Cul4B use Ddb1 as an adaptor and DCAFs (Ddb1 and Cul4-associated factors) as substrate receptors to recognize a large number of substrate proteins [24-26]. CRL4s play recognized roles in DNA repair, replication and chromatin modifications through ubiquitylation and/or mediating protein-protein interactions [27, 28].

Mammalian cells have two Eco1 orthologs, Esco1 and Esco2 [29]. Both of these have been shown to acetylate Smc3 at two evolutionarily conserved lysine residues (K105K106) [15, 30, 31]. Interestingly, Esco1 acetylates Smc3 through a mechanism

distinct from that of Esco2 [32]. Nevertheless, how the activities of Esco1 and Esco2 are controlled to establish replication-coupled sister chromatid cohesion in vertebrates has not been delineated.

In this study, we report that Cul4-Ddb1 E3 ligases function in establishing sister chromatid cohesion in human cells. Depletion of Cul4A, Cul4B or Ddb1 results in precocious sister chromatid separation. We show that Mms22L (Mms22-like), the human ortholog of yeast Mms22, the substrate receptor of Rtt101-Mms1, interacts with Ddb1. Interestingly, Esco2, not Esco1, co-immunoprecipitates with all of the subunits of $CRL4^{Mms22L}$ ligase. Dosage suppression experiments reveal that CRL4s and Esco2 are able to compensate each other in Smc3 acetylation and thereby sister chromatid cohesion in 293T cells. Through introducing interaction defective mutations, we find that Esco2 acetylates Smc3 dependent on interactions with both Cul4-Ddb1 ligases and PCNA. These data suggest that Cul4-Ddb1 ligases and PCNA contribute together to connect Esco2-dependent cohesion establishment with the replication process in human.

Results

Cul4-Ddb1 and Mms22L are required for efficient sister chromatid cohesion in human cells

Recently, we showed that fork-associated Rtt101-Mms1 ubiquitin ligases function in linking the establishment of sister chromatid cohesion with DNA replication in yeast [20]. We asked whether Cul4-Ddb1, the putative functional homolog of Rtt101-Mms1 in human cells, participate in sister chromatid cohesion as well. To test this, we

depleted Cul4A, Cul4B or Ddb1 from 293T cells using small interfering RNA (siRNA) and measured sister chromatid cohesion. Cultured cells were harvested by trypsinization to enrich for cells in mitosis. Chromosome spreads were stained with Giemsa and the morphology of the mitotic cells was analyzed (Fig 1A). We did not synchronize cells in metaphase with nocodazole since vertebrate cohesins are removed from chromosome arms in prophase allowing only cohesion of centromeres to be monitored [33]. We, however, wished to monitor cohesion not only at centromeres but also at telomeres and chromosome arms, where Rtt101-Mms1 have been shown to be required for cohesion establishment [20] (Fig 1A). In our experiments, "normal cohesion" defines the state in which both centromere and chromosome arms are closely tethered each other (i, Fig 1A), whereas arm open (ii), partially separated but still paired (also called "railroad", iii), unpaired (iv) or completely separated (v) chromatids indicate various extents of cohesion impairment. Under our experimental conditions, most chromatids in a single cell display similar morphology. We calculated the cohesion percentages as the proportion of "normal cohesion" cells (i) among total mitotic cells, where indicated. Alternatively, the percentage of cells bearing separated centromeres (iii, iv and v, Fig 1A) was used as an indicator as severe cohesion deficiency (S1 Fig). Depletion of either Cul4A or Cul4B reduced the "normal cohesion" from ~80% to ~40% (Figs 1B and 1C). The specificity of RNA interference (RNAi) was verified through complementation by over-expressing the respective proteins carrying a Flag tag. This indicates that Cul4A and Cul4B may play at least partially non-redundant roles in sister chromatid

131 cohesion. Similar results were observed for cells devoid of Ddb1, whereas the cell
132 cycle progression was not significantly affected (Figs 1D and S1A-B). These results
133 indicate that Cul4A, Cul4B and Ddb1, like their homologs in yeast, are required for
134 efficient cohesion in human cells.

135 Mms22 is one of the substrate adaptors of Rtt101-Mms1 in yeast. Mms22L, a putative
136 human ortholog of Mms22, functions together with Cul4-Ddb1 in replication-coupled
137 nucleosome assembly [34]. However, it remains unknown whether it is a DCAF to
138 date. To test this, we next co-expressed GFP-Ddb1 and Flag-Mms22L in 293T cells.
139 Flag-Mms22L was immunoprecipitated by anti-Flag antibodies from whole cell
140 extracts. As shown in Fig 1E, considerable amounts of Ddb1 co-precipitated with
141 Flag-Mms22L, arguing that Mms22L interacts with Ddb1 and is likely a new DCAF
142 of CRL4 ligases in human. Interestingly, Mms22L depletion resulted in significant
143 cohesion defects at both chromosome arms and centromeres, reminiscent of depletion
144 of other CRL4 subunits Cul4A, Cul4B or Ddb1 (Figs 1F and S1C). Taken together,
145 these data suggest that $CRL4^{Mms22L}$ ligases participate in sister chromatid cohesion in
146 human cells.

147 **$CRL4^{Mms22L}$ ligases selectively interact with Esco2**

148 To answer how CRL4s affect sister chromatid cohesion, we tested whether CRL4
149 subunits interact with the key cohesin acetyltransferases Esco1 or Esco2. We first
150 observed the cellular distribution of Esco1, Esco2, Cul4A, Cul4B or Ddb1 by
151 immunofluorescence. RFP-labelled Esco1 or Esco2 and GFP-tagged Cul4A, Cul4B or
152 Ddb1 were introduced into 293T cells. In agreement with previous observations [23,

35], Cul4B localized to nucleus, whereas Cul4A and Ddb1 distributed throughout the whole cell. Esco1 and Esco2 mainly distributed within nucleus (Figs 2A and 2B), as reported previously by other groups [29, 36].

Meanwhile, in order to obtain insight into how Esco2 is regulated, we searched for its interaction partners using affinity purification coupled mass spectrometry (AP-MS). To this end, Esco2 carrying both His6 and 5Flag tags was over-expressed in 293T cells and subjected to tandem affinity purification. Interestingly, Ddb1, together with many histone subunits and chaperones (e.g., HP1), was repeatedly detected among the co-purified proteins with Esco2-HF (Fig 3A). We then performed immunoprecipitations to corroborate the interaction through ectopically expressing Flag tagged subunit of CRL4s in 293T cells. Consistently, Esco2 clearly co-precipitated with not only Ddb1 (Fig 3B) but also other CRL4 subunits (Figs 3C and S2). On the contrary, virtually no Esco1 was detectable in the precipitates of any CRL4 subunits in all experiments carried out in parallel with Esco2 (Figs 3B-C and S2). These data indicate that CRL4 ligases might have a preferential association with Esco2.

Esco2 functions in a CRL4^{Mms22L}-dependent manner

Given the possible interaction between CRL4s and Esco2, we asked whether lack of Ddb1-Mms22L can be compensated by over-expressing Esco2. To test this, we ectopically expressed Esco2 in a Ddb1 (Fig 4A) or Mms22L depleted background (Fig 4B). Both mild and severe cohesion defects in either Ddb1 or Mms22L-depleted 293T cells were markedly rescued by over-expression of Esco2 (Figs 4A-B, S3A-B,

lane 6), indicating a potent functional interaction between Ddb1^{Mms22L} and Esco2 as well as the physical interaction documented in Fig 3. We had previously isolated a separation-of-function mutant in yeast, *eco1-LG* (L61DG63D), which shows a dramatically compromised interaction with Mms22 [20]. Interestingly, these two residues are highly conserved in Esco2 (L415G417), but not in Esco1 (S3C Fig), which correlates well with their different abilities to interact with CRL4s^{Mms22L}. Over-expression of *Esco2*-LG (*Esco2*-L415DG417D) mutant suppressed to a lesser extent than wild-type (WT) *Esco2* (Figs 4A-B, S3A-B, compare lane 7 to 6), indicating that the role of Esco2 is at least partially dependent on its interaction with Ddb1^{Mms22L}. In order to further address the contribution of the interaction of Esco2 and CRL4s in sister chromatid cohesion, we tested the dosage suppression effects in an Esco2-depleted background. In comparison to WT Esco2, expression of the interaction defective mutant *Esco2*-LG hardly displayed suppression (Figs 4C and S3D, compare lane 6 to 5). This result reinforces the argument that the interaction between Esco2 and CRL4^{Mms22L} is important for the role of Esco2 in cohesion establishment. To further support this, Cul4, Ddb1 and Mms22L are dosage suppressors of Esco2 knockdown mutant as well (Figs 4C and S3D, lanes 7-10). These results implicate that Ddb1^{Mms22L} might serve as a critical positive regulator of the cohesion function of Esco2.

Because defects in sister chromatid cohesion often activate the spindle checkpoint and result in the G_2/M arrest of the cell cycle, we then examined the proportion of M-phase cells (mitotic index). The mitotic index was very low for untreated 293T

197 cells, but increased to an average about 12% when Esco2 was depleted (Fig 4D,
198 column 2) consistent with the observations from another group [37]. The G_2/M arrest
199 induced by Esco2 knockdown was dramatically alleviated via over-expression of
200 Cul4A or Cul4B (Fig 4D, columns 6 and 7), Ddb1 (column 8) or Mms22L (column 9).
201 Taken together, these data demonstrate that the interaction between $CRL4^{Mms22L}$ and
202 Esco2 is important for Esco2 function in sister chromatid cohesion and thereby
203 mitotic progression.
204 Besides interaction with CRL4s, the activity of Eco1 is also linked with replication
205 forks through association with PCNA in yeast [19]. This notion was corroborated
206 because the cohesion defects (S3E Fig) and mitotic arrest (Fig 4D, compare lanes 10
207 and 11) in Esco2-depleted 293T cells were significantly rescued by over-expression of
208 WT PCNA, but not by an Esco-interaction defective mutant *PCNA*-A252V. Together,
209 these data suggest that both $CRL4^{Mms22L}$ and PCNA mediated interactions are critical
210 for the Esco2-dependent establishment of sister chromatid cohesion.
211 **Cul4-Ddb1 ligases participate in sister chromatid cohesion by promoting**
212 **Esco2-mediated Smc3 acetylation**
213 Given that the essential role of Eco1/Esco lies in catalyzing Smc3 acetylation during
214 cohesion establishment [13, 38], we next examined whether the dosage suppression
215 effects observed above are due to facilitating Smc3 acetylation. For this purpose,
216 Smc3 acetylation was measured in 293T cell lysates via immunoblots with an
217 antibody that specifically recognizes Smc3K105ac/K106ac. S4A Fig demonstrates
218 that the antibody recognizes an amount of Smc3ac proportional to the input protein

concentrations. Esco2-depleted cells displayed substantially reduced Smc3 acetylation (S4B Fig, compare lanes 1, 2 and 7), which was partially restored through ectopic expression of Ddb1 or Mms22L (S4B Fig, compare lanes 1, 5 and 6). Over-expression of either Cul4A or Cul4B was also capable of stimulating Smc3 acetylation to a similar extent (S4B Fig, lanes 3 and 4). These results suggest that the compensation of cohesion defects in Esco2-depleted cells by Cul4, Ddb1, or Mms22L over-expression may be achieved through enhancing Smc3 acetylation.

Next, we determined whether CRL4s directly participate in regulating Smc3 acetylation. Depletion of each subunit of CRL4s led to moderately compromised Smc3 acetylation (Figs 5A and S4C- S4E), indicating that $CRL4s^{Mms22L}$ are required for efficient Esco2-dependent Smc3 acetylation. Meanwhile, the protein levels of both Esco enzymes were not significantly affected (Fig 5A, descending panels 3 and 4), suggesting that Cul4-Ddb1-Mms22L unlikely regulate the expression and/or protein turnover of Esco1 and Esco2.

To further validate the role of CRL4s in Smc3 acetylation, we then asked whether inhibition of HDAC8 is able to restore compromised Smc3 acetylation caused by $CRL4^{Mms22L}$ -depletion. Since HDAC8 is the deacetylase of Smc3 [39], we treated proliferating cells with the HDAC8 inhibitor, PCI-34051. In the presence of PCI-34051, Smc3 acetylation increased markedly in both WT and Esco2-depleted cells (Fig 5B, lanes 1-4), as reported previously [32]. There is a similar increase in the Smc3ac level when Ddb1 and Mms22L were depleted individually (lanes 5-8). Nevertheless, Shirahige's group shows that PCI-34051 is not able to restore the

241 Smc3ac levels caused by compromised Pds5A-Pds5B-Esco1 branch [32]. This
242 supports that Ddb1 and Mms22L function in the Esco2-catalyzed Smc3 acetylation
243 pathway, which can be reversed by HDAC8. Taken together, these data reinforce the
244 notion that CRL4^{Mms22L} ligases modulate the activity of Esco2 on Smc3 acetylation.

245 **Both CRL4s and PCNA help to stabilize Esco2 on chromatin**

246 Next, we directly tested whether the regulation of CRL4s on the Esco2 activity
247 depends on their interactions shown in Fig 3. To this end, we constructed several
248 *Esco2* alleles defective in either CRL4s-binding (*Esco2*-LG) or PCNA-binding
249 (*Esco2*-PIP) according to highly conserved sites from yeast to human (Fig 6A). To
250 obtain a catalytic-deficient enzyme, we also introduced the missense mutation
251 W539G in Esco2, which occurs frequently in Roberts Syndrome (RBS) patients [40].
252 Indeed, the W539G allele showed a substantially decrease in Smc3 acetylation (Fig
253 6B, lane 5), in agreement with its location within the acetyltransferase domain.
254 *Esco2*-LG exhibited a significant decrease in Smc3 acetylation and cohesion efficacy
255 to a similar extent as the catalytic-deficient W539 allele (Fig 6B, lane 3), indicating
256 that CRL4s-mediated interaction is crucial for Esco2 operating on Smc3. Similarly, a
257 PCNA-interaction defective allele, *Esco2*-PIP, reduced Smc3 acetylation and cohesion
258 efficacy as well (lane 2). Interestingly, when we combined both mutations on Esco2
259 (Esco2-LG-PIP), we found a synergistic loss of Smc3 acetylation and cohesion (Fig
260 6B, lane 4). These data suggest that the function of Esco2 is cooperatively regulated
261 through its dual interaction with both CRL4^{Mms22L} and PCNA.

262 Since both CRL4^{Mms22L} and PCNA associate with replication forks, we then analyzed

263 the contribution of Ddb1 and PCNA to the chromatin recruitment of Esco2.
264 Chromatin fractions were prepared from the 293T cells transfected with siRNAs
265 specific to Ddb1 or PCNA. Depletion of either Ddb1 or PCNA led to moderately
266 reduced amounts of Esco2 on chromatin (Fig 6C, lanes 6 and 7). The combinational
267 depletion of Ddb1 and PCNA only posed a subtle effect on the total Esco2 levels (Fig
268 6C, WCE, lane 4). Nevertheless, a clear synergistic loss of Esco2 on chromatin was
269 observed (CHR, lane 8). Consistently, the level of acetylated Smc3 largely reduced
270 whereas the total Smc3 protein on chromatin remained nearly unaffected (Fig 6C,
271 descending panels 3 and 4). Meanwhile, the chromatin-associated Esco1 level only
272 displayed a mild change (Fig 6C, lane 8, panel 2). In good agreement with this, only
273 when Ddb1 and PCNA depletions were combined, dramatic cell death was observed
274 by live cell staining (Fig 6D). These data suggest a cooperative mechanism for CRL4s
275 and PCNA to properly target the essential cohesin acetyltransferase Esco2 on its
276 substrate Smc3, which contributes to the coupling between the establishment of sister
277 chromatid cohesion and replication fork progression in human cells (Fig 6E).

278 ## Discussion

279 How sister chromatid cohesion is established in mammals remains largely unclear.
280 Here we have identified an evolutionarily conserved mechanism of CRL4 ubiquitin
281 ligases, together with PCNA, in regulation of DNA replication-coupled cohesion
282 establishment in human cells.

283 The essential step to establish cohesion is Smc3 acetylation by Eco1 and Esco in yeast
284 and human, respectively [13-15]. Precise control of the reaction is required for this

essential cellular process. One of the main findings of this study is that human CRL4^{Mms22L} ligases exclusively interact with and preferentially regulate Esco2. Despite that both Esco1 and Esco2 catalyze acetylation of Smc3, their temporal regulation is distinct [32, 37, 41]. Esco1 acetylates Smc3 in a Pds5-dependent manner before and after DNA replication [37], whereas Esco2 is believed to function during S phase. Our findings provide molecular details of how Esco2 is controlled in a DNA replication-coupled fashion by dual interaction with CRL4^{Mms22L} and PCNA in human cells.

During the revision of this manuscript, Peters's group reported that Esco2 is recruited to chromatin via direct association with MCM, the core of eukaryotic replicative helicase Cdc45-Mcm2-7-GINS [42]. It's worth noting that the contributions of MCM, PCNA and CRL4s to Esco2 regulation are not mutually exclusive. A very interesting finding in their work is that Esco2 binds MCM predominantly in the context of chromatin regardless that there are largely excess amounts of MCM in nucleoplasm [42]. Even among the abundant chromatin-loaded MCM rings, only a small portion of these are activated and assembled into replication forks [43, 44]. How Esco2 is specifically recognized by the activated MCM and travels with replication fork has therefore not been addressed yet. The interactions of Esco2 with PCNA and CRL4^{Mms22L} identified previously and in this study [19], albeit relatively weak or transient, may contribute to the preferential association of Esco2 with the activated MCMs on replication fork. Intriguingly, in HeLa cells, Mms22L-TONSL bind MCM as well as replication-coupled H3.1-H4 [45-50]. Therefore, it will be of great interest

to test the functional interplay among these fork-associated factors in future.

In addition to these interactions, CRL4s have been found to be involved in multiple replication-coupled chromatid events. For instance, Cul4-Ddb1 (Rtt101-Mms1) ubiquitylates histone H3-H4, which elicits the new histone hand-off from Asf1 to other chaperones for chromatin reassembly in both yeast and human cells [34]. Another CRL4, $CRL4^{WDR23}$, ubiquitylates SLBP to activate histone mRNA processing and expression during DNA replication [51]. Further studies are needed to illustrate the details of crosstalk among these replication-coupled events, for instance, nucleosome assembly and cohesion establishment÷in human cells.

Over-expression of Cul4, Ddb1 and Mms22L has been reported to correlate with lung and esophageal carcinogenesis [52], implicating them as key genome caretakers. Mutations in *Esco2* gene cause Roberts Syndromes with a predisposition to cancer [40]. The functional interplay between Cul4-Ddb1 and Esco2 identified here will shed new light for us to understand the etiology of these human diseases.

Materials and methods

Cell culture and RNAi

HEK293T cells were cultured in DMEM media supplemented with 10% fetal bovine serum (FBS, Gibco) at 37℃ with 5% CO_2. For RNAi experiments, cells were transfected with 80 nM siRNAs using Lipofectamine 3000 (Invitrogen) for 48 h following the manufacturer's instructions. Over-expression plasmid or control plasmid for target genes was transferred into the cells when necessary. For HDAC8 inhibition experiments, 6.25 μM PCI-34051 (Selleckchem) was applied 3 h before

329 harvest. Immunoblotting with specific antibodies was used to confirm the
330 downregulation of the targets. The sequences of siRNA oligos used in this study are
331 listed in Table 1. All siRNA oligos were synthesized by Sangon Biotech, China.

332 **Plasmid construction**

333 Trizol reagent (CWBIO) was used to isolate total RNA according to the
334 manufacturer's instructions. cDNA was synthesized using reverse transcriptase
335 (Promega). Full length genes studied were inserted to the prk5-Flag, GFP or mCherry
336 vectors [53]. The prk5-Flag vector was kindly provided by Dr. Jun Tang (China
337 Agricultural University) and Flag was replaced by GFP or mCherry when necessary.

338 **Chromosome spreads**

339 Chromosome spreads were performed as described in [54], with minor modifications.
340 In brief, cultured cells were harvested by trypsinization and then 75 mM KCl was
341 used as hypotonic treatment. Cells were fixed with methanol and acetic acid (3:1)
342 three times and then dropped onto the slides. After half an hour, cells were stained
343 with 0.05% Giemsa (Merck) for 10 min at room temperature. Images were captured
344 using a Leica microscope equipped with a 100×/NA1.3 oil objective. The incidence of
345 sister chromatid separation was determined from at least 200 mitotic cells and all
346 experiments were repeated at least three times. In our experimental conditions, almost
347 all chromosomes within a single cell display similar cohesion defects. Total cohesion
348 defects were counted as cells exhibiting precocious separation of both arms and
349 centromeres, while *CEN* cohesion defects shown in the Supporting Figures were
350 calculated for the percentages of cells bearing separated centromeres among mitotic

cells.

Cell extract, Immunoprecipitation and Immunoblotting

Cells were washed twice with PBS. To obtain whole cell extracts for immunoblotting, cells were resuspended with RIPA buffer (50 mM Tris-HCl, 250 mM NaCl, 1% TritonX-100, 0.25% Sodium deoxycholate, 0.05% SDS, 1 mM DTT) and lysed on ice for 20 min. For immunoprecipitation experiments, cells were resuspended in lysis buffer (50 mM Tris-HCl, 150 mM NaCl, 1% NP-40, 5 mM EDTA, 10% glycerin) and incubated on ice for 20 min, then sonicated for 30 sec. For each sample, 250 μg total protein was incubated with anti-Flag agarose for 1.5 h at 4 ℃, then washed five times with lysis buffer. All of the samples were run on sodium dodecyl sulfate polyacrylamide gel electrophoresis (SDS-PAGE) and transferred to PVDF membranes. Signals were detected with specific antibodies using eECL Western Blot Kit (CWBIO).

Affinity purification coupled to mass spectrometry (AP-MS)

Esco2-HF was purified from whole cell extracts by anti-Flag M2 (Sigma) and Ni^{2+} affinity gels successively. Nonspecific bound proteins were removed by washing with 0.25 μg/μl Flag peptide. Bound fraction was eluted by 2 μg/μl Flag peptide and 300 mM imidazole, respectively. An untagged cell line and Esco1-HF were subjected to the same procedure as controls. The final eluates were analyzed by mass spectrometry analysis (Q Exactive™ Hybrid Quadrupole-Orbitrap Mass Spectrometer, Thermo Fisher). The procedures were repeated three times for both Esco2-HF and Esco1-HF to identify the different interactors of Esco2 and Esco1.

373 **Fluorescence stain**

374 Cells were grown in cover glasses placed into 6-well plates (Nunc) and transfected
375 with plasmids using Lipofectamine 3000 (Invitrogen) for 24 h according to the
376 instructions. After being fixed with 4% paraformaldehyde, cells were stained with 1
377 μg/ml DAPI for 5 min at room temperature. Images were captured with a
378 laser‐confocal microscope (DMi8; Leica Microsystems).

379 **Antibodies**

380 Antibodies used in this work were as below: Esco1 (Abcam, ab180100), Esco2
381 (Abcam, ab86003), Cul4A (proteintech, 14851-1-AP), Cul4B (Proteintech,
382 12916-1-AP), Ddb1 (Abcam, ab9194), Mms22L (Abcam, ab181047), Smc3
383 (BETHYL, A300-060A), acetylated Smc3 (Merck, MABE1073), Orc2 (CST, #4736),
384 Tubulin (MBL, PM054) and PCNA (Santa Cruz, sc-56).

385 ## Acknowledgments

386 We thank Dr. Judith L. Campbell for improving the manuscript, Drs. Cong Liu,
387 Jun Tang, Qun He and members of the Lou lab for discussion. We are also grateful to
388 the anonymous reviewers for constructive suggestions.

389 ## Author Contributions

390 H.L., J.J.Z. and Q.C. conceived and designed the overall project; H.S. conducted
391 most experiments with the help from J.X.Z. and J.J.Z.; Z.L. helped in mass spectra
392 analysis; H.L. H.S. and Q.C. wrote the manuscript with input and editing from all of
393 the authors.

394 ## Competing interest statement

395 The authors declare no competing financial interests.

References

1. Onn I, Heidinger-Pauli JM, Guacci V, Unal E, Koshland DE. Sister chromatid cohesion: a simple concept with a complex reality. Annu Rev Cell Dev Biol. 2008;24:105-29. https://doi.org/10.1146/annurev.cellbio.24.110707.175350 PMID: 18616427

2. Peters J-M, Tedeschi A, Schmitz J. The cohesin complex and its roles in chromosome biology. Genes Dev. 2008;22(22):3089-114. https://doi.org/10.1101/gad.1724308 PMID: 19056890

3. Uhlmann F. A matter of choice: the establishment of sister chromatid cohesion. EMBO Rep. 2009;10(10):1095-102. https://doi.org/10.1038/embor.2009.207 PMID: 19745840

4. Leman A, Noguchi E. Linking Chromosome Duplication and Segregation via Sister Chromatid Cohesion. In: Noguchi E, Gadaleta MC, editors. Cell Cycle Control. Methods in Molecular Biology. 1170: Springer New York; 2014. p. 75-98.

5. Marston AL. Chromosome Segregation in Budding Yeast: Sister Chromatid Cohesion and Related Mechanisms. Genetics. 2014;196(1):31-63. https://doi.org/10.1534/genetics.112.145144 PMID: 24395824

6. Zheng G, Yu H. Regulation of sister chromatid cohesion during the mitotic cell cycle. Sci China Life Sci. 2015;58:1089-98. https://doi.org/10.1007/s11427-015-4956-7 PMID: 26511516

7. Nasmyth K, Haering CH. The structure and function of SMC and kleisin complexes. Annu Rev Biochem. 2005;74:595-648.

https://doi.org/10.1146/annurev.biochem.74.082803.133219 PMID: 15952899

8. Losada A, Hirano T. Dynamic molecular linkers of the genome: the first decade of SMC proteins. Genes Dev. 2005;19(11):1269-87. https://doi.org/10.1101/gad.1320505 PMID: 15937217

9. Nasmyth K, Haering CH. Cohesin: its roles and mechanisms. Annu Rev Genet. 2009;43:525-58. https://doi.org/10.1146/annurev-genet-102108-134233 PMID: 19886810

10. Losada A. Cohesin in cancer: chromosome segregation and beyond. Nat Rev Cancer. 2014;14(6):389-93. https://doi.org/10.1038/nrc3743 PMID: 24854081

11. Ocampo-Hafalla MT, Uhlmann F. Cohesin loading and sliding. J Cell Sci. 2011;124(5):685-91. https://doi.org/10.1242/jcs.073866 PMID: 21321326

12. Sherwood R, Takahashi TS, Jallepalli PV. Sister acts: coordinating DNA replication and cohesion establishment. Genes & Development. 2010;24(24):2723-31. https://doi.org/10.1101/gad.1976710 PMID: 21159813

13. Rolef Ben-Shahar T, Heeger S, Lehane C, East P, Flynn H, Skehel M, et al. Eco1-dependent cohesin acetylation during establishment of sister chromatid cohesion. Science. 2008;321(5888):563-6. https://doi.org/10.1126/science.1157774 PMID: 18653893

14. Unal E, Heidinger-Pauli JM, Kim W, Guacci V, Onn I, Gygi SP, et al. A molecular determinant for the establishment of sister chromatid cohesion. Science. 2008;321(5888):566-9. https://doi.org/10.1126/science.1157880 PMID: 18653894

15. Zhang J, Shi X, Li Y, Kim B-J, Jia J, Huang Z, et al. Acetylation of Smc3 by Eco1 Is Required for S Phase Sister Chromatid Cohesion in Both Human and Yeast. Mol Cell. 2008;31(1):143-51. https://doi.org/10.1016/j.molcel.2008.06.006 PMID:

18614053

16. Rowland BD, Roig MB, Nishino T, Kurze A, Uluocak P, Mishra A, et al. Building Sister Chromatid Cohesion: Smc3 Acetylation Counteracts an Antiestablishment Activity. Molecular Cell. 2009;33(6):763-74. https://doi.org/10.1016/j.molcel.2009.02.028 PMID: 19328069

17. Uhlmann F, Nasmyth K. Cohesion between sister chromatids must be established during DNA replication. Curr Biol. 1998;8(20):1095-102. PMID: 9778527

18. Skibbens RV. Sticking a fork in cohesin – it's not done yet! Trends Genet. 2011;27(12):499-506. https://doi.org/10.1016/j.tig.2011.08.004 PMID: 21943501

19. Moldovan GL, Pfander B, Jentsch S. PCNA controls establishment of sister chromatid cohesion during S phase. Mol Cell. 2006;23(5):723-32. https://doi.org/10.1016/j.molcel.2006.07.007 PMID: 16934511

20. Zhang J, Shi D, Li X, Ding L, Tang J, Liu C, et al. Rtt101-Mms1-Mms22 coordinates replication-coupled sister chromatid cohesion and nucleosome assembly. EMBO J. 2017;18:1294-305. https://doi.org/10.15252/embr.201643807 PMID: 28615292

21. Sarikas A, Hartmann T, Pan Z-Q. The cullin protein family. Genome Biology. 2011;12(4):220. https://doi.org/10.1186/gb-2011-12-4-220 PMID: 21554755

22. Zaidi IW, Rabut G, Poveda A, Scheel H, Malmstrom J, Ulrich H, et al. Rtt101 and Mms1 in budding yeast form a CUL4(DDB1)-like ubiquitin ligase that promotes replication through damaged DNA. EMBO J. 2008;9(10):1034-40. https://doi.org/10.1038/embor.2008.155 PMID: 18704118

464 23. Hannah J, Zhou P. Distinct and overlapping functions of the cullin E3 ligase
465 scaffolding proteins CUL4A and CUL4B. Gene. 2015;573(1):33-45.
466 https://doi.org/10.1016/j.gene.2015.08.064 PMID: 26344709
467 24. Zimmerman ES, Schulman BA, Zheng N. Structural assembly of cullin-RING
468 ubiquitin ligase complexes. Curr Opin Struct Biol. 2010;20(6):714-21.
469 https://doi.org/10.1016/j.sbi.2010.08.010 PMID: 20880695
470 25. Lee J, Zhou P. DCAFs, the Missing Link of the CUL4-DDB1 Ubiquitin Ligase.
471 Mol Cell. 2007;26(6):775-80. https://doi.org/10.1016/j.molcel.2007.06.001 PMID:
472 17588513
473 26. Lydeard JR, Schulman BA, Harper JW. Building and remodelling Cullin–RING
474 E3 ubiquitin ligases. EMBO Rep. 2013;14(12):1050-61.
475 https://doi.org/10.1038/embor.2013.173 PMID: 24232186
476 27. Jackson S, Xiong Y. CRL4s: the CUL4-RING E3 ubiquitin ligases. Trends
477 Biochem Sci. 2009;34(11):562-70. https://doi.org/10.1016/j.tibs.2009.07.002 PMID:
478 19818632
479 28. Iovine B, Iannella ML, Bevilacqua MA. Damage-specific DNA binding protein 1
480 (DDB1): a protein with a wide range of functions. Int J Biochem Cell Biol.
481 2011;43(12):1664-7. https://doi.org/10.1016/j.biocel.2011.09.001 PMID: 21959250
482 29. Hou F, Zou H. Two human orthologues of Eco1/Ctf7 acetyltransferases are both
483 required for proper sister-chromatid cohesion. Mol Biol Cell. 2005;16(8):3908-18.
484 https://doi.org/10.1091/mbc.e04-12-1063 PMID: 15958495
485 30. Kouznetsova E, Kanno T, Karlberg T, Thorsell AG, Wisniewska M, Kursula P, et

al. Sister Chromatid Cohesion Establishment Factor ESCO1 Operates by Substrate-Assisted Catalysis. Structure. 2016;24:789-96. https://doi.org/10.1016/j.str.2016.03.021 PMID: 27112597

31. Rivera-Colon Y, Maguire A, Liszczak GP, Olia AS, Marmorstein R. Molecular Basis for Cohesin Acetylation by Establishment of Sister Chromatid Cohesion N-acetyltransferase ESCO1. J Biol Chem. 2016;29:26468-77. https://doi.org/10.1074/jbc.M116.752220 PMID: 27803161

32. Minamino M, Ishibashi M, Nakato R, Akiyama K, Tanaka H, Kato Y, et al. Esco1 Acetylates Cohesin via a Mechanism Different from That of Esco2. Curr Biol. 2015;25(13):1694-706. https://doi.org/10.1016/j.cub.2015.05.017 PMID: 26051894

33. Waizenegger IC, Hauf S, Meinke A, Peters J-M. Two Distinct Pathways Remove Mammalian Cohesin from Chromosome Arms in Prophase and from Centromeres in Anaphase. Cell. 2000;103(3):399-410. PMID: 11081627

34. Han J, Zhang H, Zhang H, Wang Z, Zhou H, Zhang Z. A Cul4 E3 ubiquitin ligase regulates histone hand-off during nucleosome assembly. Cell. 2013;155(4):817-29. https://doi.org/10.1016/j.cell.2013.10.014 PMID: 24209620

35. Zou Y, Mi J, Cui J, Lu D, Zhang X, Guo C, et al. Characterization of Nuclear Localization Signal in the N Terminus of CUL4B and Its Essential Role in Cyclin E Degradation and Cell Cycle Progression. J Biol Chem. 2009;284(48):33320-32. https://doi.org/10.1074/jbc.M109.050427 PMID: 19801544

36. Whelan G, Kreidl E, Wutz G, Egner A, Peters JM, Eichele G. Cohesin acetyltransferase Esco2 is a cell viability factor and is required for cohesion in

508 pericentric heterochromatin. EMBO J. 2011;31(1):71-82.
509 https://doi.org/10.1038/emboj.2011.381 PMID: 22101327
510 37. Alomer RM, da Silva EML, Chen J, Piekarz KM, McDonald K, Sansam CG, et al.
511 Esco1 and Esco2 regulate distinct cohesin functions during cell cycle progression.
512 Proc Natl Acad Sci. 2017;114:9906-11. https://doi.org/10.1073/pnas.1708291114
513 PMID: 28847955
514 38. Beckouët F, Hu B, Roig MB, Sutani T, Komata M, Uluocak P, et al. An Smc3
515 Acetylation Cycle Is Essential for Establishment of Sister Chromatid Cohesion. Mol
516 Cell. 2010;39(5):689-99. https://doi.org/10.1016/j.molcel.2010.08.008 PMID:
517 20832721
518 39. Deardorff MA, Bando M, Nakato R, Watrin E, Itoh T, Minamino M, et al.
519 HDAC8 mutations in Cornelia de Lange syndrome affect the cohesin acetylation
520 cycle. Nature. 2012;489:313. https://www.nature.com/articles/nature11316
521 PMID:22885700
522 40. Vega H, Trainer AH, Gordillo M, Crosier M, Kayserili H, Skovby F, et al.
523 Phenotypic variability in 49 cases of ESCO2 mutations, including novel missense and
524 codon deletion in the acetyltransferase domain, correlates with ESCO2 expression
525 and establishes the clinical criteria for Roberts syndrome. J Med Genet.
526 2010;47(1):30-7. https://doi.org/10.1136/jmg.2009.068395 PMID: 19574259
527 41. Kawasumi R, Abe T, Arakawa H, Garre M, Hirota K, Branzei D. ESCO1/2's roles
528 in chromosome structure and interphase chromatin organization. Genes Dev.
529 2017;31:2136-50. https://doi.org/10.1101/gad.306084.117 PMID: 29196537

530 42. Ivanov MP, Ladurner R, Poser I, Beveridge R, Rampler E, Hudecz O, et al. The
531 replicative helicase MCM recruits cohesin acetyltransferase ESCO2 to mediate
532 centromeric sister chromatid cohesion. EMBO J. 2018:e97150.
533 https://doi.org/10.15252/embj.201797150 PMID: 29930102
534 43. Ge XQ, Jackson DA, Blow JJ. Dormant origins licensed by excess Mcm2–7 are
535 required for human cells to survive replicative stress. Genes Dev.
536 2007;21(24):3331-41. https://doi.org/10.1101/gad.457807 PMID: 18079179
537 44. Ibarra A, Schwob E, Méndez J. Excess MCM proteins protect human cells from
538 replicative stress by licensing backup origins of replication. Proc Natl Acad Sci.
539 2008;105(26):8956-61. https://doi.org/10.1073/pnas.0803978105 PMID: 18579778
540 45. Duro E, Lundin C, Ask K, Sanchez-Pulido L, MacArtney TJ, Toth R, et al.
541 Identification of the MMS22L-TONSL complex that promotes homologous
542 recombination. Mol Cell. 2010;40(4):632-44.
543 https://doi.org/10.1016/j.molcel.2010.10.023 PMID: 21055984
544 46. O'Donnell L, Panier S, Wildenhain J, Tkach JM, Al-Hakim A, Landry MC, et al.
545 The MMS22L-TONSL complex mediates recovery from replication stress and
546 homologous recombination. Mol Cell. 2010;40(4):619-31.
547 https://doi.org/10.1016/j.molcel.2010.10.024 PMID: 21055983
548 47. O'Connell BC, Adamson B, Lydeard JR, Sowa ME, Ciccia A, Bredemeyer AL, et
549 al. A genome-wide camptothecin sensitivity screen identifies a mammalian
550 MMS22L-NFKBIL2 complex required for genomic stability. Mol Cell.
551 2010;40(4):645-57. https://doi.org/10.1016/j.molcel.2010.10.022 PMID: 21055985

552 48. Piwko W, Olma MH, Held M, Bianco JN, Pedrioli PG, Hofmann K, et al.
553 RNAi-based screening identifies the Mms22L-Nfkbil2 complex as a novel regulator
554 of DNA replication in human cells. EMBO J. 2010;29(24):4210-22.
555 https://doi.org/10.1038/emboj.2010.304 PMID: 21113133
556 49. Campos Eric I, Smits Arne H, Kang Y-H, Landry S, Escobar Thelma M, Nayak S,
557 et al. Analysis of the Histone H3.1 Interactome: A Suitable Chaperone for the Right
558 Event. Mol Cell. 2015;60(4):697-709. https://doi.org/10.1016/j.molcel.2015.08.005
559 PMID: 26527279
560 50. Saredi G, Huang H, Hammond CM, Alabert C, Bekker-Jensen S, Forne I, et al.
561 H4K20me0 marks post-replicative chromatin and recruits the TONSL–MMS22L
562 DNA repair complex. Nature. 2016;534:714-8. https://doi.org/10.1038/nature18312
563 PMID: 27338793
564 51. Brodersen Mia ML, Lampert F, Barnes Christopher A, Soste M, Piwko W, Peter
565 M. CRL4(WDR23)-Mediated SLBP Ubiquitylation Ensures Histone Supply during
566 DNA Replication. Mol Cell. 2016;62(4):627-35.
567 https://doi.org/10.1016/j.molcel.2016.04.017 PMID: 27203182
568 52. Nguyen MH, Ueda K, Nakamura Y, Daigo Y. Identification of a novel oncogene,
569 MMS22L, involved in lung and esophageal carcinogenesis. Int J Oncol.
570 2012;41(4):1285-96. https://doi.org/10.3892/ijo.2012.1589 PMID: 22895565
571 53. Li C, Peng Q, Wan X, Sun H, Tang J. C-terminal motifs in promyelocytic
572 leukemia protein isoforms critically regulate PML nuclear body formation. J Cell Sci.
573 2017;130(20):3496-506. http://jcs.biologists.org/content/130/20/3496 PMID:

28851805

54. Giménez-Abián JF, Lane AB, Clarke DJ. Analyzing Mitotic Chromosome Structural Defects After Topoisomerase II Inhibition or Mutation. In: Drolet M, editor. DNA Topoisomerases: Methods and Protocols. New York, NY: Springer New York; 2018. p. 191-215.

581 **Table 1: The sequences of siRNA oligos**

Target gene	sequences of siRNA oligos
Esco1	5’-CCAGUGUUGAAAGACAAAUACUUCA-3’
	5’-GGACAAAGCUACAUGAUAG-3’
Esco2	5’-GACCCAACACCAGAUGGCAAGUUAU-3’
	5’-ACAGAAGAGUUUAACUGCUAAGUAU-3’
Cul4A	5’-GAAGCUGGUCAUCAAGAAC-3’
	5’-GACAAUCCGAAUCAGUACC-3’
Cul4B	5’-AAGCCUAAAUUACCAGAAA-3’
	5’-AGAUAAGGUUGACCAUAUA-3’
Ddb1	5’-CGUUGACAGUAAUGAACAAGGCUCC-3’
	5’-CCUGUUGAUUGCCAAAAAC-3’
Mms22L	5’-UCACAAAGUCCUUGGAAUA-3’
	5’-AAGACUUGCUGUUGCGAUA-3’
PCNA	5’-GGAGGAAGCUGUUACCAUA-3’
	5’-CGGUGACACUCAGUAUGUC-3’
Mock	5’-UUCUCCGAACGUGUCACGU-3’

582

583 **Figure legends**

584 **Fig 1. Knockdown of Cul4-Ddb1-Mms22L causes severe cohesion defects.**

585 (A) Representative morphologies of human chromosome spreads stained with Giemsa.
586 Closed sister chromatids (i) indicates normal cohesion, while loose sister chromatids
587 (arm opened, loosely paired, unpaired and completely separated, ii-v) indicate
588 different extents of cohesion defects. We have only rarely observed that chromosomes
589 within one cell display different morphologies. In order to reflect the physiological
590 status of chromosome morphologies, cells were not synchronized. At least 200 mitotic
591 cells were enriched and harvested via trypsin digestion for each experiment. The
592 percentage of cells with closed sister chromatids among the total mitotic cells (i.e.,
593 normal cohesion %) was quantified from at least three independent experiments.
594 (B-D) Cohesion defects caused by depletion of Cul4A (B), Cul4B (C) and Ddb1 (D).
595 293T cells were transfected with siRNAs specific to Cul4A, Cul4B and Ddb1 for 48 h.
596 A plasmid expressing the indicated Flag-tagged protein was transferred into the cells
597 after 6 h for the complementation assay. The trysinized cells were fixed with methanol
598 and acetic acid (3:1) for three times and then stained with Giemsa. More than 200
599 mitotic cells per RNAi experiment were scored; the results of at least three
600 independent biological experiments were summarized in the histogram. The cohesion
601 percentage of each RNAi sample was compared with that of mock or add-back using
602 student's *t*-test, **P<0.01. The efficiency of siRNA and complementation of Cul4A,
603 Cul4B, Ddb1 or Mms22L was detected via immunoblots against the indicated
604 antibodies.

(E) Ddb1 co-precipitates with Mms22L. *Flag*, *Flag-Mms22L* and *GFP*, *GFP-Ddb1* plasmids were transferred into 293T cells. After IP experiments, Mms22L and Ddb1 were detected with antibodies against Flag and GFP, respectively. Tubulin was probed as a loading control.

(F) Mms22L depletion leads to compromised cohesion as well. Quantification of the cohesion percentage was performed as described above. See Supporting S1 Fig for the *CEN* cohesion defect results.

Fig 2. Esco2 co-localizes with Cul4 and Ddb1.

(A) Localization of Esco2, Cul4A, Cul4B and Ddb1. 293T cells were co-transferred with *RFP-Esco2* plasmids and *GFP*, *GFP-Cul4A*, *GFP-Cul4B*, or *GFP-Ddb1* plasmids. After 24 h, nuclei were stained with DAPI. Pictures were captured with a laser-confocal microscope. RFP and GFP images were merged with (lane 6) or without DAPI (lane 5).

(B) Esco1 does not co-localize with CRL4s. 293T cells were co-transferred with *RFP-Esco1* plasmids and *GFP*, *GFP-Cul4A*, *GFP-Cul4B*, or *GFP-Ddb1* plasmids. Fluorescence microscopy was conducted as described above.

Fig 3. Preferential interaction between CRL4s^{Mms22L} and Esco2.

(A) Ddb1 is repeatedly co-purified with Esco2. 293T cells were co-transferred with *Esco2-HF* plasmid. After tandem affinity purification, proteins in the final elution were analyzed by MS. Cells expressing Esco1-HF were conducted as a control.

(B, C) Esco2, but not Esco1, co-immunoprecipitates with Cul4A-Cul4B-Ddb1-Mms22L. *GFP*, *GFP-Esco1*, *GFP-Esco2* and *Flag-Ddb1* (B) or

627 *Flag-Cul4B* (C) were co-expressed in 293T cells. Flag-IP experiments were
628 performed as described in Fig 1E. The asterisks indicate non-specific reacting bands.
629 See Supporting S2 Figs for the data of *Flag-Cul4A* and *Flag-Mms22L*
630 immunoprecipitation experiments.

631 **Fig 4. Functional interaction between CRL4s^{Mms22L} and Esco2.**

632 (A) Over-expression of Esco1, Esco2 or PCNA partially suppresses a cohesion defect
633 in Ddb1 knockdown cells, while over-expression of *Esco2-LG* mutant does not.
634 Immunoblots of Ddb1, Esco1, Esco2, PCNA and Tubulin were shown below each
635 column. The statistical significance was calculated via student's *t*-test, ** P<0.01; *
636 P<0.05. The results of at least three independent biological experiments were
637 summarized in the histogram. See Supporting S3A Fig for the corresponding *CEN*
638 cohesion defect results.

639 (B) Esco1, Esco2 or PCNA over-expression partially compensates a SCC defect
640 caused by Mms22L knockdown, while over-expression of *Esco2-LG* mutant does not.
641 Immunoblots of Mms22L, Esco1, Esco2, PCNA and Tubulin are shown below each
642 column. The statistical significance was calculated via student's *t*-test, ** P<0.01; *
643 P<0.05. The results of at least three independent biological experiments were
644 summarized in the histogram. See Supporting S3B Fig for the corresponding *CEN*
645 cohesion defect results.

646 (C) Over-expression of Cul4A, Cul4B, Ddb1, or Mms22L partially suppresses the
647 SCC defect caused by Esco2 knockdown, while over-expression of an E3-interaction
648 defective mutant, or *Esco2*-LG (L415DG417D) mutant has no effect. Esco2 was

649 knocked down by siRNA in 293T cells, then Flag-tagged Esco1, Esco2, *Esco2*-LG,
650 Cul4A, Cul4B, Ddb1, or Mms22L were overexpressed after siRNA delivery for 6 h.
651 The percentage of cells in cohesion was determined as in Fig 1. Immunoblots of
652 Esco2, Flag and Tubulin from each RNAi experiment are shown below the
653 corresponding column. The statistical significance was calculated via student's *t*-test,
654 *** P<0.001; ** P<0.01. The results of at least three independent biological
655 experiments were summarized in the histogram. See Supporting S3D Fig for the
656 corresponding *CEN* cohesion defect results. See Supporting S3E Fig for the results of
657 PCNA and PCNA-A252V alleles.
658 (D) Over-expression of Cul4A, Cul4B, Ddb1, Mms22L or PCNA suppresses the M
659 phase arrest caused by Esco2 knockdown. The portion of cells in the M phase among
660 total cells was counted after Hoechst 33342 staining. The statistical significance was
661 calculated via student's *t*-test, *** P<0.001, n: the total cell number counted. The
662 results of at least three independent biological experiments were summarized.
663 **Fig 5. Cul4A/Cul4B-Ddb1-Mms22L are required for Esco2-dependent Smc3**
664 **acetylation**
665 (A) Knockdown of Cul4-Ddb1-Mms22L leads to reduced Smc3 acetylation. Smc3
666 acetylation was analyzed in the siRNA-transfected cells as above. The statistical
667 significance from at least three independent repeats was calculated via student's *t*-test,
668 *P<0.05. The results of at least three independent biological experiments were
669 summarized in the histogram. See S4A Fig for the linear ranges of quantitation
670 analysis of immunoblots, S4B Fig for the dosage suppression results of

671 Esco2-depleted cells, and S4C- S4E for biological repeats.

672 (B) Inhibition of deacetylase HDAC8 restores Smc3ac levels in Ddb1 and Mms22L –
673 depleted cells. The indicated cells were cultured and treated by PCI-34051 for 2 h
674 before collection and Giemsa analysis. Mitotic cells with normal cohesion were
675 counted as described in Fig 1. The statistical significance was calculated via student's
676 *t*-test, ** P<0.01.

677 **Fig 6. Both CRL4s and PCNA mediated interactions are required for stabilizing**
678 **Esco2 on chromatin.**

679 (A) The interaction motifs of Eco1/Esco2 with PCNA and CRL4s are evolutionarily
680 conserved from yeast to human. The amino acid sequences of Eco1/Esco2 from the
681 indicated organisms were aligned by CLC Genomics Workbench 3.

682 (B) *Esco2* mutants display compromised Smc3 acetylation and thereby cohesion
683 establishment. *Esco2* alleles: PIP, *Esco2*-Q374AI376AI377A; LG,
684 *Esco2*-L415DG417D; PIP-LG, *Esco2*-Q374AI376AI377A-L415DG417D.
685 Quantitation from three biological repeats is shown for Smc3ac (middle) and cohesion
686 efficiency (lower). The statistical significance was calculated via student's *t*-test,
687 *P<0.05，**P<0.01. The results of at least three independent biological experiments
688 were summarized in the histogram.

689 (C) Ddb1 and PCNA are required for the chromatin association of Esco2. Chromatin
690 fractions were prepared from cells transfected with the Ddb1 or PCNA siRNAs. Orc2
691 served as a loading control of the chromatin-enriched fraction (CHR). Three
692 independent biological experiments were performed and one of the results was shown.

693 (D) Combined depletion of Ddb1 and PCNA caused cell death. Cells were stained
694 with Coomassie brilliant blue 48 h after transfection with the indicated siRNAs. Three
695 independent biological experiments were performed and one of the results was shown.
696 (E) A co-regulation model of Esco2 by CRL4s and PCNA in human cells.
697 As replication fork proceeding during S phase, Esco2 is recruited via interactions with
698 fork components including PCNA and $CRL4^{Mms22L}$ ligases. This is required for
699 efficient Smc3 acetylation of the pre-loaded cohesin ring, which triggers the
700 establishment of cohesion between two newly synthesized sister chromatids.
701

Fig.1

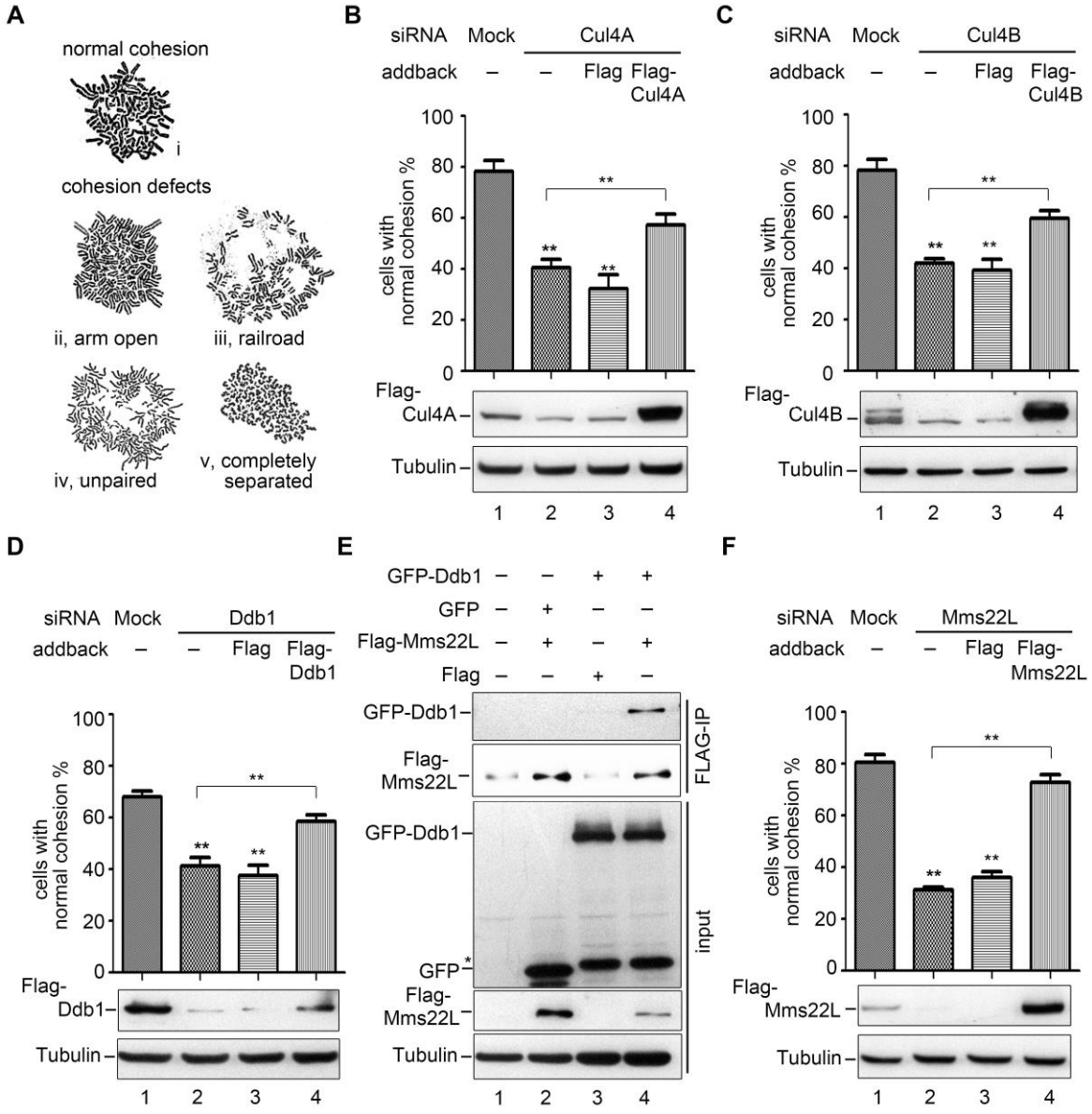

705 Fig. 2

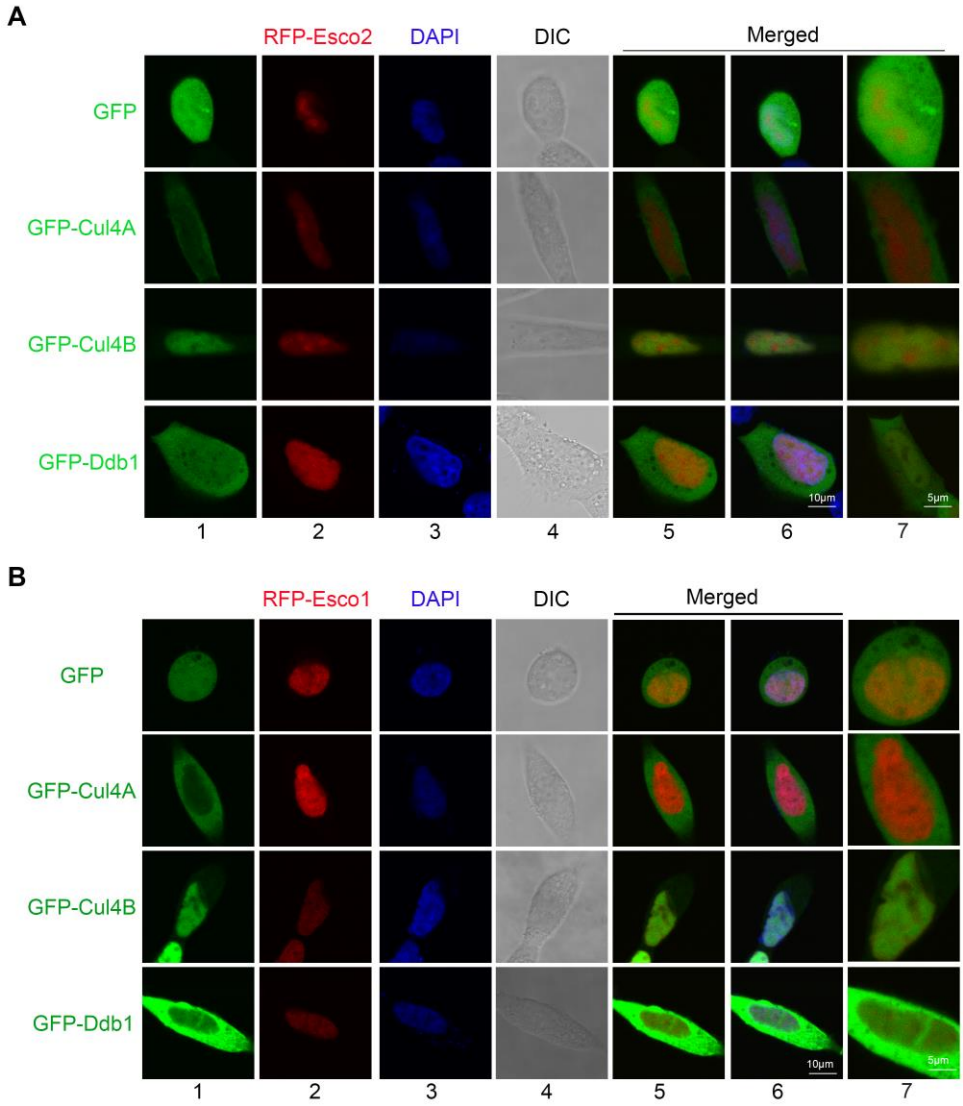

706
707

708 Fig.3

A

Protein	Number of matches	Number of sequences	Score
ESCO2	264	49	6926
DDB1	14	12	111
H2AY	15	9	186
H2A	11	3	174
H1X	5	3	168
H3.1	24	8	148
H3	19	7	115
H2AW	6	4	58
HOYHC3	5	4	69
RBBP7	5	4	57
HP1B3	6	5	53

B

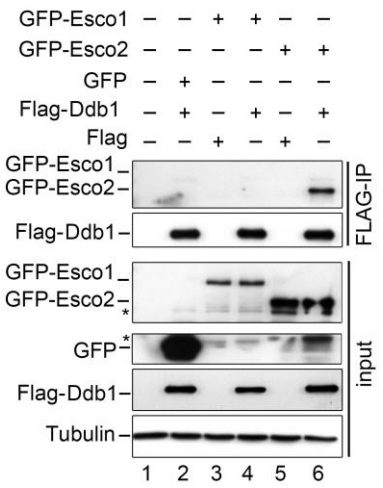

C

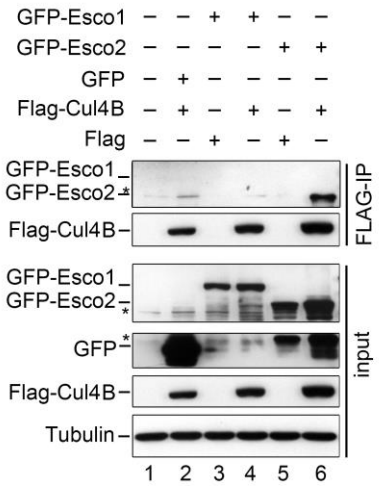

709

710

711 Fig.4

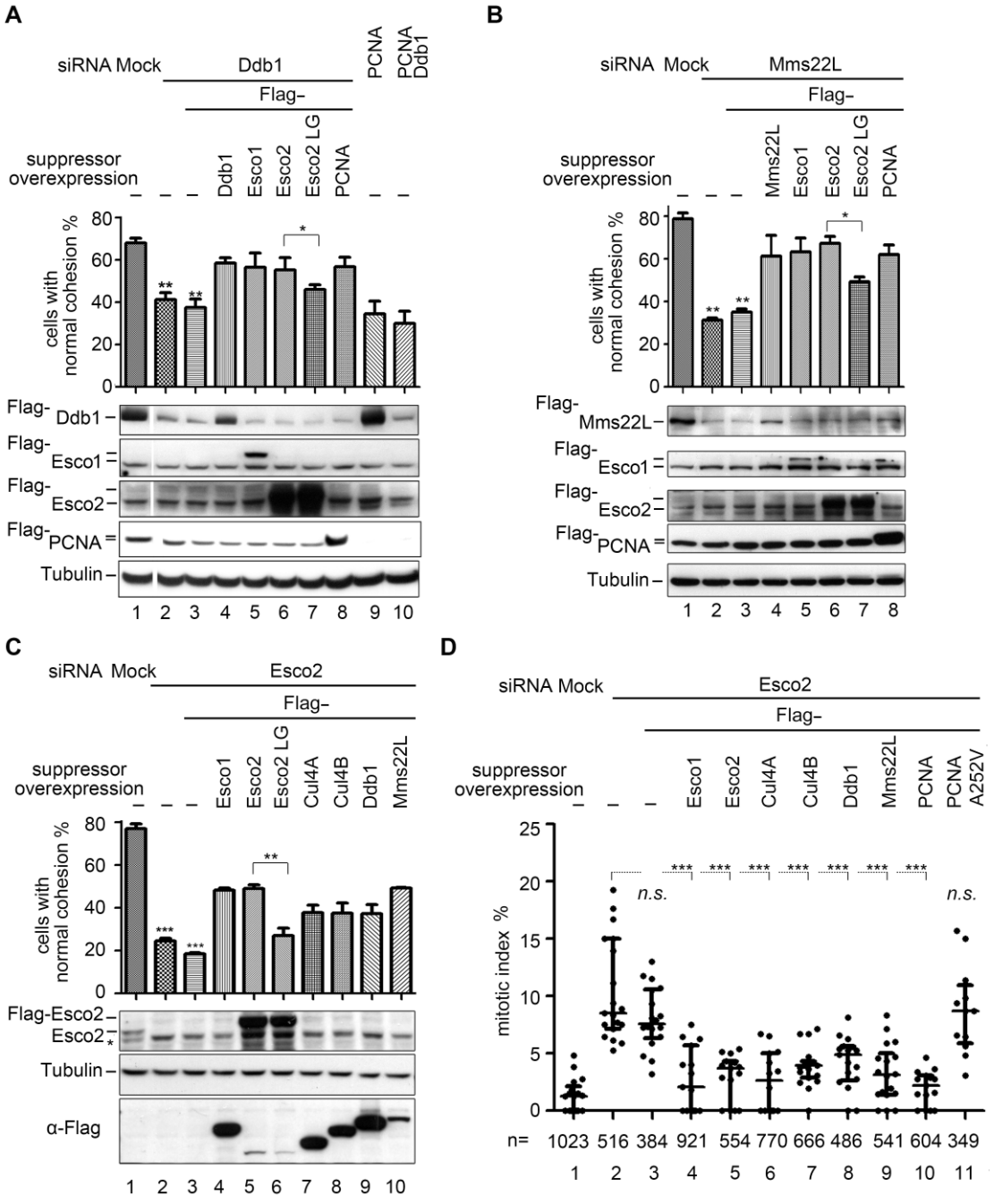

712

713

714 Fig.5

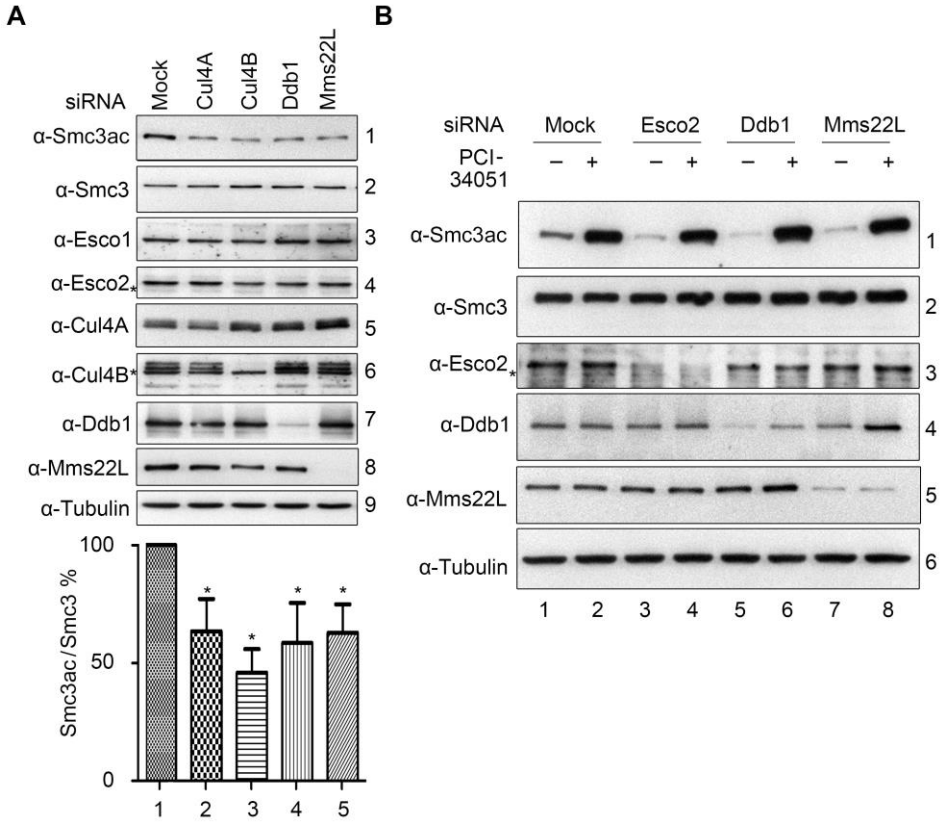

715
716

717 Fig.6

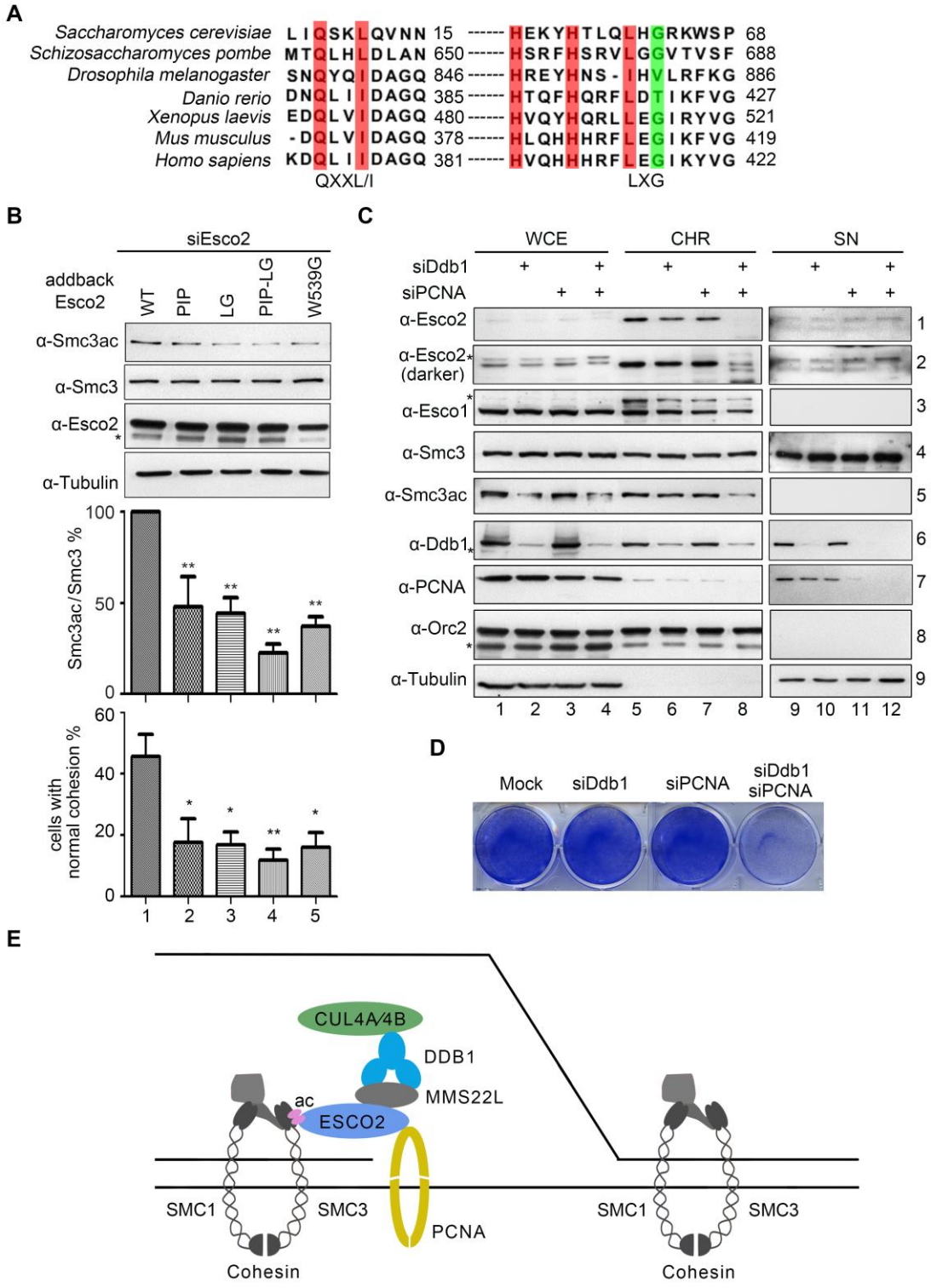

718